Astron. Astrophys. 201, 138–142 (1988)

ASTRONOMY AND ASTROPHYSICS

Effects of CO molecules on the outer solar atmosphere. Dynamical models with opacity distribution functions

D. Muchmore[1], R.L. Kurucz[2], and P. Ulmschneider[1]

[1] Institut für Theoretische Astrophysik, Universität Heidelberg, Im Neuenheimer Feld 561, D-6900 Heidelberg, Federal Republic of Germany
[2] Harvard-Smithsonian Center for Astrophysics, 60 Garden Street, Cambridge, MA 02138, USA

Received September 11, 1987; accepted January 26, 1988

Summary. Carbon monoxide can be an important cooling agent in late-type stars. We expand on our previous theoretical work by extending the frequency set used in the radiation calculations, employing opacity distribution functions for the infrared bands of CO and 19 frequency points for the H^- continuum. We find that the net cooling rate due to CO decreases by a factor of about 3 due to the large optical depths in the line cores. The influence of the 2.2 μm CO band is small compared to the effect of the 4.6 μm band. We again find an atmospheric structure with a sharp drop of the temperature in the outer photosphere where CO cooling sets in. This temperature drop occurs higher in the atmosphere and is less steep than in the simpler models but is nevertheless steep enough to be convectively unstable. When CO cooling sets in, surface temperatures drop to very low values ($T < 3000$ K) for radiative equilibrium models even without including the effects of other molecules.

Key words: solar atmosphere – CO molecules – hydrodynamics – radiation transfer

1. Introduction

Tsuji (1968) first pointed out that molecules in the atmospheres of cool late-type stars lead to strong surface cooling. This effect has been discussed by a variety of other workers using models with varying degrees of accuracy (Johnson, 1973; Gustafsson et al., 1975). This discussion has been intensified in recent years by the discovery of Ayres and Testerman (1981; see also Ayres et al., 1986) that even the Sun seems to show signs of very cool surface layers when one looks at CO lines in the 4.6 μm fundamental rotation-vibration band. The inferred brightness temperatures in the cores of strong lines seen near the solar limb amount to $\approx$3700 K, in contrast to the minimum temperatures of some 4300 K which are inferred from optical and UV spectral indicators such as the wings of the Ca II H and K or Mg II h and k lines. Those observations have received further support from recent work by Ayres et al. (1986) and from suggestions of similar effects elsewhere, such as in solar OH bands at 10 μm (Deming et al., 1984) and in Arcturus (Heasley et al., 1978). The observations indicate (Ayres, 1981) that the cooling by CO molecules might lead to horizontally separated regions of the solar atmosphere with drastically different temperatures. In addition Kneer (1983) pointed out that the formation and dissociation of molecules under such conditions are autocatalytic reactions, since, for instance, the formation of a CO molecule leads to more effective radiative cooling and hence to further molecule formation.

Our time-dependent radiation hydrodynamic work (Muchmore and Ulmschneider, 1985, hereafter MU) confirmed that for stars with $T_{\rm eff} < 5800$ K CO cooling leads to very cold outer layers. In this treatment the radiation field was computed using two frequency points, one to represent the H^- continuum and the other to model the 4.6 μm CO band. That work showed moreover that the extent of the cold outer layer also depends on the amount of mechanical (acoustic wave) heating. In addition Muchmore (1986) discovered that there is a range of $T_{\rm eff}$ where the atmosphere is no longer uniquely determined by the boundary conditions but depends on the previous time-history. If in a state with a cold outer CO layer the effective temperature $T_{\rm eff}$ in the atmosphere is raised from 5400 K to 5800 K the atmosphere retains its cold outer layer. At $T_{\rm eff} > 5800$ K the atmosphere abruptly changes into the hot state where the cold CO layer no longer exists. On the other hand if $T_{\rm eff}$ is lowered from 5900 K down to 5600 K the atmosphere retains its hot state and at 5600 K abruptly changes into the cold state. In the present work, by greatly increasing the number of frequency points and using opacity distribution functions to describe in much greater detail both the 4.6 μm and 2.2 μm CO bands, we want to investigate the validity of our two frequency point simulations and want to learn whether these important cooling effects are not artifacts of an oversimplistic treatment. Section 2 describes our method of computation, Sect. 3 the model calculations while Sect. 4 gives our conclusions.

2. Method of computation

The model calculations reported here are time-dependent solutions of the hydrodynamical equations including radiative transfer using the same methods as MU. The hydrodynamical code has been described by Ulmschneider et al. (1977, 1978) and the method used for radiative transfer by Kalkofen and Ulmschneider (1977) and MU.

Aside from the inclusion of the 2.2 μm band the difference between the current method and that of MU lies in the frequency points chosen. Previously we took two frequency points: one in

Send offprint requests to: P. Ulmschneider

the optical band with a Rosseland mean opacity and one in the infrared with a Planck mean over the 4.6 μm band of CO. In the present calculations, we use a total of 19 frequency points from 6 μm to 3000 Å, using the H^- continuum opacity calculated as in Schmitz et al. (1985), with the exception that the IR frequency points have been shifted to include and bracket the 2.2 and 4.6 μm CO bands. One frequency point each is used to represent the two IR bands of CO. At these frequencies, we calculated the radiative transfer using opacity distribution functions (ODF's).

The CO opacities were computed using the spectrum synthesis program described by Kurucz and Avrett (1981) to produce the line absorption coefficient spectrum including only $^{12}C^{16}O$ vibration-rotation lines. The line positions were determined from the energy levels of Mantz et al. (1975) and the gf values were derived from the work of Kirby-Docken and Liu (1978). An artificial model was used consisting of solar abundance gas at 25 temperatures ranging from 2000 to 6800 K and at the pressures 1000 and 10000 dyn cm^{-2}. The abundances and pressures were specified to produce a reasonable pressure broadening for the temperature minimum region. A 1 km s^{-1} microturbulent velocity was assumed. The spectra were calculated for the bandpasses 2.28–2.80 μm and 4.29–6.20 μm with a point spacing $\lambda/\Delta\lambda$ of $5\,10^5$. After the absorption coefficient spectra were computed, they were divided by the CO number density per gram to obtain the cross section per particle. This opacity was statistically sampled (Kurucz, 1979) to produce a 1000 point distribution function. The 1000 points in the distribution function were averaged in log cross section to obtain the few points actually used in the calculations.

We have performed a series of tests to determine a suitable subsample of the ODF's. A compromise must be reached between the desire for accuracy which is best served by the inclusion of many ODF pickets and the need for computational speed which demands the fewest points necessary since the radiative transfer equation must typically be solved several times in iterating the hydrodynamical variables to their solution at each time step. The accuracy of various choices for pickets of the ODF's were compared. Using both a model nearly in equilibrium in the cool phase and a model far from equilibrium with transient temperature gradients, we find that the radiative losses (or gains) can be represented accurately with 7 or more pickets when they are concentrated toward the line core regions. With fewer points we obtain increasingly large deviations from the accurate solution.

These tests indicate that even with as few as 3 pickets for the ODF's it is possible to roughly approximate the radiative transfer in an important band. Such a small subset could profitably be used for time-dependent calculations which encounter temperatures cool enough for CO to form but which do not seek a detailed modelling of the temperature minimum region. In the neighborhood of 3 pickets, increasing or decreasing the number of points has substantial effects on the quality of the results. Using fewer points is very poor; adding a few more points improves the quality, but then adding still more points makes little additional difference. With 7 pickets, the solutions for $D(z)$ differ only insignificantly from those with more pickets. For the model calculations of the next sections, 7 pickets have been used. The opacity distribution functions and weightings for this choice are given in Table 1 where the first and last pickets represent the line wing and the line core, respectively. For temperatures below 2600 K, due to the small populations of excited states in the 2.2 μm band, the opacity sampling procedure did not yield meaningful results and we assigned the opacity in these cases an arbitrary small value 10^{-30}.

3. Model calculations

To evaluate the accuracy of our simplified two frequency point method (henceforth called old method) we have recalculated the solar cases of MU with $T_{\rm eff}=5600$ K and 5770 K. For the $T_{\rm eff}=5600$ K case and for the radiative damping functions D of CO and H^-, Fig. 1 shows a comparison of the old method with the method using many frequency points (henceforth called new method). The radiative damping function D (erg $g^{-1}s^{-1}K^{-1}$ cf.

Table 1a. Logarithms of opacity distribution functions for CO in cm^2 per CO molecule for the 4.6 μm (top) and 2.2 μm (bottom) bands as function of temperature for pressure $p=10^3$ dyn cm^{-2}. The weights of the seven pickets are given in the top line

T(K)	0.5	0.3	0.1	0.05	0.025	0.015	0.010
2000	-24.588	-22.432	-21.554	-20.835	-20.131	-19.331	-18.256
2200	-24.345	-22.357	-21.463	-20.738	-20.026	-19.228	-18.242
2400	-24.144	-22.278	-21.370	-20.641	-19.922	-19.135	-18.229
2600	-23.977	-22.199	-21.281	-20.547	-19.824	-19.055	-18.222
2800	-23.844	-22.131	-21.202	-20.460	-19.734	-18.987	-18.222
3000	-23.741	-22.074	-21.135	-20.382	-19.650	-18.936	-18.229
3200	-23.658	-22.023	-21.073	-20.305	-19.572	-18.893	-18.235
3400	-23.588	-21.975	-21.013	-20.233	-19.500	-18.859	-18.249
3600	-23.528	-21.929	-20.956	-20.163	-19.434	-18.833	-18.259
3800	-23.475	-21.885	-20.902	-20.096	-19.378	-18.811	-18.274
4000	-23.429	-21.842	-20.849	-20.034	-19.329	-18.795	-18.292
4200	-23.390	-21.802	-20.797	-19.974	-19.287	-18.781	-18.310
4400	-23.358	-21.763	-20.747	-19.918	-19.250	-18.771	-18.327
4600	-23.335	-21.726	-20.698	-19.866	-19.218	-18.765	-18.346
4800	-23.321	-21.691	-20.652	-19.818	-19.191	-18.760	-18.364
5000	-23.314	-21.656	-20.605	-19.772	-19.169	-18.760	-18.383
5200	-23.311	-21.621	-20.561	-19.730	-19.149	-18.759	-18.403
5400	-23.310	-21.588	-20.516	-19.690	-19.131	-18.761	-18.423
5600	-23.310	-21.561	-20.473	-19.655	-19.118	-18.765	-18.442
5800	-23.310	-21.544	-20.431	-19.622	-19.107	-18.770	-18.464
6000	-23.310	-21.538	-20.393	-19.594	-19.098	-18.775	-18.479
6300	-23.310	-21.537	-20.362	-19.568	-19.092	-18.783	-18.505
6400	-23.310	-21.537	-20.349	-19.549	-19.089	-18.793	-18.526
6600	-23.310	-21.537	-20.349	-19.536	-19.089	-18.805	-18.551
6800	-23.310	-21.537	-20.346	-19.523	-19.080	-18.802	-18.555

T(K)	0.5	0.3	0.1	0.05	0.025	0.015	0.010
2000	-30.000	-30.000	-30.000	-30.000	-30.000	-30.000	-30.000
2200	-30.000	-30.000	-30.000	-30.000	-30.000	-30.000	-30.000
2400	-30.000	-30.000	-30.000	-30.000	-30.000	-30.000	-30.000
2600	-26.603	-24.104	-23.010	-22.230	-21.535	-20.935	-20.309
2800	-26.479	-23.969	-22.864	-22.080	-21.398	-20.852	-20.297
3000	-26.380	-23.851	-22.731	-21.943	-21.283	-20.786	-20.289
3200	-26.300	-23.742	-22.607	-21.814	-21.185	-20.729	-20.283
3400	-26.224	-23.641	-22.492	-21.694	-21.101	-20.682	-20.281
3600	-26.145	-23.548	-22.383	-21.585	-21.028	-20.641	-20.280
3800	-25.848	-23.462	-22.281	-21.488	-20.965	-20.605	-20.278
4000	-25.707	-23.381	-22.184	-21.402	-20.911	-20.578	-20.277
4200	-25.566	-23.307	-22.093	-21.325	-20.863	-20.553	-20.275
4400	-25.420	-23.237	-22.007	-21.255	-20.822	-20.533	-20.274
4600	-25.368	-23.174	-21.927	-21.195	-20.787	-20.516	-20.272
4800	-25.349	-23.116	-21.853	-21.141	-20.756	-20.501	-20.271
5000	-25.341	-23.062	-21.781	-21.095	-20.730	-20.489	-20.270
5200	-25.339	-23.016	-21.714	-21.052	-20.706	-20.480	-20.268
5400	-25.339	-22.981	-21.651	-21.013	-20.684	-20.472	-20.267
5600	-25.339	-22.960	-21.594	-20.979	-20.668	-20.465	-20.265
5800	-25.339	-22.951	-21.542	-20.950	-20.654	-20.460	-20.264
6000	-25.339	-22.949	-21.500	-20.923	-20.640	-20.455	-20.262
6200	-25.339	-22.949	-21.477	-20.902	-20.631	-20.452	-20.261
6400	-25.339	-22.949	-21.477	-20.898	-20.629	-20.452	-20.261
6600	-30.000	-30.000	-30.000	-30.000	-30.000	-30.000	-30.000
6800	-30.000	-30.000	-30.000	-30.000	-30.000	-30.000	-30.000

Table 1b. Same as Table 1a however for the pressure $p=10^4$ dyn/cm^{-2}

T(K)	0.5	0.3	0.1	0.05	0.025	0.015	0.010
2000	-23.941	-21.762	-20.980	-20.389	-19.810	-19.170	-18.263
2200	-23.664	-21.672	-20.895	-20.311	-19.734	-19.093	-18.260
2400	-23.438	-21.591	-20.818	-20.239	-19.664	-19.025	-18.255
2600	-23.258	-21.518	-20.749	-20.172	-19.597	-18.968	-18.258
2800	-23.108	-21.451	-20.686	-20.109	-19.533	-18.922	-18.264
3000	-22.983	-21.389	-20.628	-20.052	-19.473	-18.887	-18.279
3200	-22.877	-21.333	-20.576	-19.998	-19.417	-18.858	-18.293
3400	-22.785	-21.281	-20.527	-19.946	-19.367	-18.837	-18.311
3600	-22.706	-21.233	-20.482	-19.896	-19.323	-18.820	-18.329
3800	-22.636	-21.189	-20.441	-19.849	-19.286	-18.808	-18.348
4000	-22.575	-21.149	-20.402	-19.804	-19.253	-18.800	-18.366
4200	-22.523	-21.114	-20.367	-19.763	-19.225	-18.794	-18.388
4400	-22.477	-21.083	-20.336	-19.725	-19.200	-18.791	-18.408
4600	-22.439	-21.057	-20.309	-19.691	-19.180	-18.791	-18.425
4800	-22.408	-21.035	-20.284	-19.661	-19.164	-18.791	-18.443
5000	-22.387	-21.016	-20.261	-19.633	-19.150	-18.795	-18.461
5200	-22.376	-21.000	-20.238	-19.608	-19.138	-18.798	-18.480
5400	-22.373	-20.984	-20.215	-19.583	-19.127	-18.802	-18.498
5600	-22.373	-20.969	-20.191	-19.561	-19.119	-18.808	-18.519
5800	-22.373	-20.957	-20.164	-19.538	-19.112	-18.816	-18.540
6000	-22.373	-20.949	-20.136	-19.518	-19.108	-18.825	-18.562
6200	-22.373	-20.945	-20.108	-19.498	-19.104	-18.835	-18.593
6400	-22.373	-20.945	-20.087	-19.482	-19.103	-18.848	-18.614
6600	-22.373	-20.945	-20.080	-19.472	-19.104	-18.859	-18.638
6800	-22.373	-20.945	-20.078	-19.469	-19.107	-18.870	-18.658

T(K)	0.5	0.3	0.1	0.05	0.025	0.015	0.010
2000	-30.000	-30.000	-30.000	-30.000	-30.000	-30.000	-30.000
2200	-30.000	-30.000	-30.000	-30.000	-30.000	-30.000	-30.000
2400	-25.883	-23.542	-22.719	-22.136	-21.563	-21.006	-20.367
2600	-25.733	-23.417	-22.606	-22.021	-21.442	-20.924	-20.357
2800	-25.604	-23.304	-22.497	-21.907	-21.333	-20.854	-20.347
3000	-25.497	-23.203	-22.397	-21.798	-21.239	-20.796	-20.340
3200	-25.410	-23.115	-22.308	-21.694	-21.156	-20.746	-20.336
3400	-25.339	-23.037	-22.227	-21.598	-21.083	-20.703	-20.334
3600	-25.281	-22.968	-22.150	-21.509	-21.019	-20.667	-20.332
3800	-25.231	-22.905	-22.075	-21.428	-20.964	-20.635	-20.329
4000	-25.189	-22.847	-22.003	-21.355	-20.916	-20.608	-20.327
4200	-25.128	-22.793	-21.932	-21.289	-20.873	-20.584	-20.325
4400	-24.769	-22.745	-21.863	-21.229	-20.834	-20.564	-20.322
4600	-24.649	-22.701	-21.796	-21.176	-20.801	-20.548	-20.320
4800	-24.521	-22.661	-21.735	-21.128	-20.772	-20.534	-20.318
5000	-24.511	-22.626	-21.675	-21.085	-20.747	-20.521	-20.315
5200	-24.506	-22.594	-21.619	-21.046	-20.725	-20.512	-20.313
5400	-24.505	-22.568	-21.566	-21.010	-20.705	-20.504	-20.310
5600	-24.505	-22.549	-21.517	-20.979	-20.689	-20.497	-20.308
5800	-24.505	-22.536	-21.471	-20.952	-20.676	-20.493	-20.306
6000	-24.505	-22.528	-21.430	-20.928	-20.665	-20.489	-20.303
6200	-24.505	-22.524	-21.393	-20.908	-20.657	-20.487	-20.301
6400	-24.505	-22.522	-21.363	-20.892	-20.652	-20.487	-20.301
6600	-24.505	-22.522	-21.358	-20.886	-20.655	-20.492	-20.301
6800	-24.505	-22.522	-21.358	-20.886	-20.655	-20.492	-20.301

Kalkofen and Ulmschneider, 1977) is defined as

$$D=-\frac{\Phi}{\rho T}, \tag{1}$$

where Φ (erg cm^{-3}s^{-1}) is the net radiative cooling rate, ρ the density and T the temperature. That Fig. 1 shows a radiative equilibrium model is seen by the fact that the total damping function D is zero. Except for the heights above 800 km this model is based on a balance between H^- heating and CO 4.6 μm band cooling. Figure 1 shows that below 700 km height the inclusion of the $\Delta v=2$ band at 2.2 μm has little apparent effect on the behavior of the model, contributing cooling only in deeper layers around optical depth $\tau 5000 \simeq 1$, where it's influence is readily compensated by heating in the optical band. At layers above 800 km however the 2.2 μm band is the main source of heating,

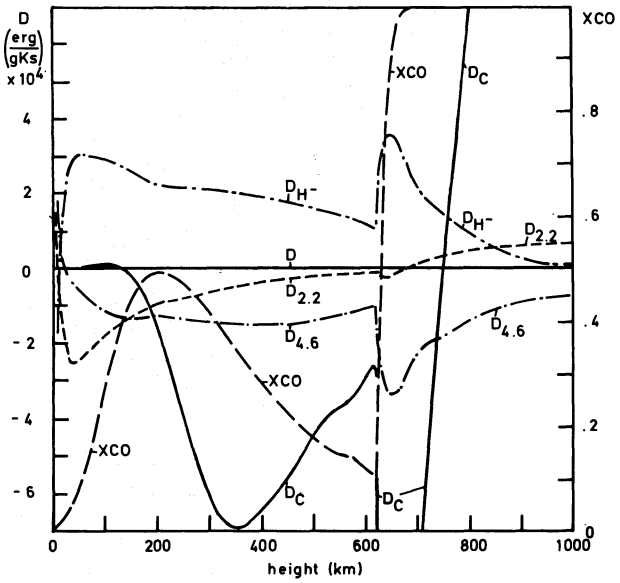

Fig. 1. Solar radiative equilibrium model with $T_{\rm eff}=5600$ K five hours after time-dependent computations which include CO have been started from the same initial pure H^- radiative equilibrium model. The radiative damping functions $D_{4.6}$, $D_{2.2}$ (erg g^{-1}K^{-1}s^{-1}) of the 4.6, 2.2 μm CO bands for the new method are indicated together with D_{H^-} for H^-. D_C is for the 4.6 μm CO band computed with the old method. XCO is the relative concentration of CO

which is due to the low opacity in this band which causes the mean intensity to be produced at low heights where the temperature is high. In addition, Fig. 1 shows the radiative damping function D_C of the 4.6 μm band computed for the same model, but now using the old method. It is seen that in the new method the amount of CO cooling is reduced by about a factor of about 3 which is due to the large opacity of the line cores which reduces the amount of energy flowing in the band and thus leads to decreased radiative losses. That D_C becomes strongly positive above 750 km height is similar to the behaviour of the 2.2 μm band. Here CO becomes a heating source because the outer layers of the ODF radiative equilibrium model are too cold for the old method.

Critical temperatures where non-unique solutions exist for the same $T_{\rm eff}$ (cf. Muchmore, 1986) have also been found using opacity distribution functions. Starting with a 5600 K radiative equilibrium model and raising $T_{\rm eff}$ in steps to 6200 K resulted in radiative equilibrium models with cold CO layers. At $T_{\rm eff}=6300$ K a hot model began to form. While starting with a hot 6200 K model and lowering $T_{\rm eff}$ we found that at $T_{\rm eff}=5700$ K a cold CO layer began to form. Non-unique solutions are thus met between about $T_{\rm eff}=5800$ K and 6200 K.

Figure 2 shows a comparison of the temperature dependence of the new and old methods in a radiative equilibrium atmosphere with $T_{\rm eff}=5600$ K. It is seen that with ODF's one has again a rapid temperature drop caused by CO, falling to even lower temperatures. However it is less steep that with the old method. The drop now occurs 200 km higher. This is a consequence of the concentration of most of the CO opacity into line cores; molecular cooling occurs efficiently only in the outer layers where the line cores become optically thin. Figure 2 also shows a comparison for the dynamical steady state models of $T_{\rm eff}=5770$ K which include

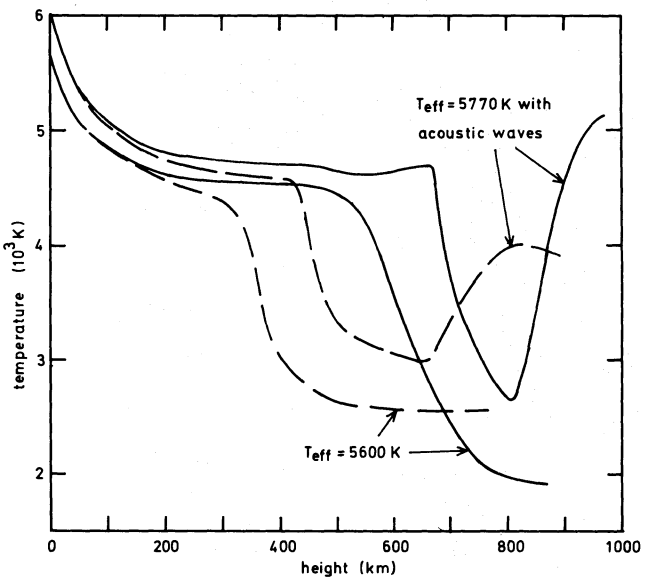

Fig. 2. Temperatures of solar radiative equilibrium models with $T_{\rm eff}$ = 5600 K which include CO. Also shown are models with $T_{\rm eff}$ = 5770 K which include CO and a small acoustic flux. The models are computed using the old (dashed) and new (solid) methods (see text)

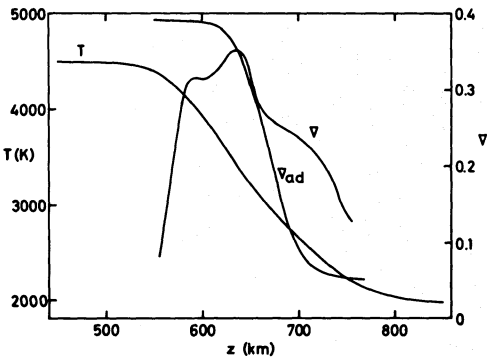

Fig. 3. Temperature and temperature gradients in the $T_{\rm eff}$ = 5600 K radiative equilibrium model using CO opacity distribution functions

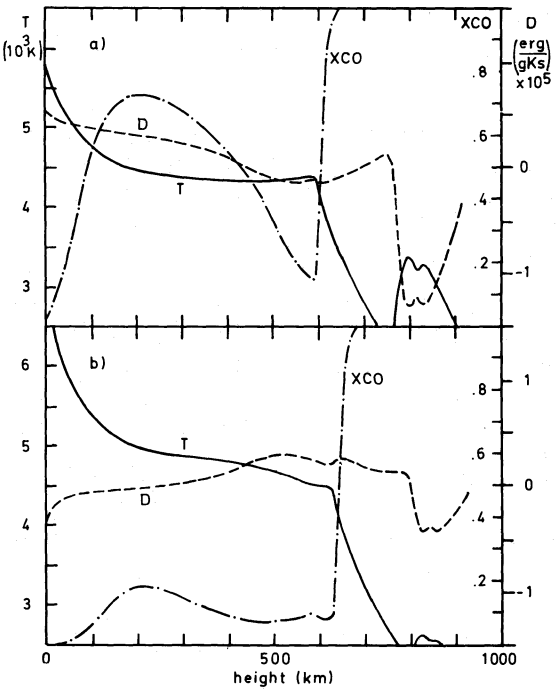

Fig. 4. Phases of the solar atmosphere subjected to a radiation field oscillating in time as $T_{\rm eff} = 5600 + 300 \sin(2\pi t/P)$ K with a period of P = 20 min. Panel a) shows the model at time 158.3 min, panel b) at time = 166.1 min

mechanical heating (with a small acoustic wave flux of 1 10^7 erg cm^{-2} s^{-1}). It is seen that the qualitative behaviour found with the old method is not much changed. The inclusion of mechanical heating (here by acoustic shock formation) limits the vertical extent of the cold CO region. More mechanical heating will consequently decrease the width of the cold region up to the point where the CO layer can be suppressed entirely with sufficient mechanical heating.

Figure 3 shows that despite the greatly reduced steepness of the temperature drop in the CO layer we find that convective instability due to H_2 formation still develops as has been pointed out by Kneer (1983). This demonstrates that some aspects of the problem can only be studied by two or three-dimensional treatments (cf. Steffen and Muchmore, 1988).

As the temperature variations across convective granules is of the order of 300 K (corresponding to a granular contrast of 21%, Bray et al., 1984, p. 46) it is interesting to simulate the effect of a varying background radiative flux due to the finite lifetime of granules. Figure 4 shows a calculation with a sinusoidal variation of $T_{\rm eff}$ around a mean of 5600 K with an amplitude of 300 K and a period of 20 min. Here we have doubled the temperature amplitude to enhance the effect and have neglected the geometrical effect of increased merging of radiative flux from hot and cold granular areas with height. A comparison of Figs. 4a and 4b which are about 180 degrees out of phase shows that the temperature oscillation mainly affects the lower hot layers of the atmosphere up to the height where CO cooling sets in. The height and shape of the CO temperature drop is not much affected by the temperature variation.

4. Conclusions

Using opacity distribution functions for the $\Delta v = 1$ and $\Delta v = 2$ IR vibration-rotation bands of the CO molecule, we have calculated dynamical models of the solar atmosphere. Qualitatively, these models resemble the simpler two-frequency models of MU, the quantitative differences are:

1) Due to optical depth effects in the line cores, CO is less effective as a coolant than we previously estimated. The difference amounts to about a factor of 3, so that time-dependent phenomena driven by molecular cooling occur more slowly by that factor. The 2.2 μm band is negligible relative to the 4.6 μm band except for the coolest parts of the models. Here other opacity sources such as metal lines, which we have neglected would have a considerable influence.

2) Surface temperatures in the cool phase models are somewhat cooler than previously estimated. For realistic models other molecules should be included.

3) The drop from photospheric temperatures to the refrigerated surface temperatures occurs less steeply than before,

but it is still steep enough so that in its cooler layers, where the formation of H_2 begins, the radiative temperature gradient is convectively unstable.

4) The CO temperature drop occurs about 200 km higher than before due to the concentration of opacity in the line cores.

5) The critical temperatures for differentiating between the cool phase and the warm phase (with and without molecules, respectively) in surface layers occurs near the solar effective temperature.

We conclude, based on the present results, that for the investigation of gas-dynamical models of cool stars, the simple (old) method described by MU for the IR CO band gives the correct physics in most cases, especially if the radiative losses in this band are scaled by a factor of about 1/3. When accuracy is important, our calculations indicate that fair results can be obtained using an opacity distribution function with as few as 3 pickets, though at least 7 are necessary for good results.

Acknowledgements. We want to acknowledge generous support by the Sonderforschungsbereich 132.

References

Ayres, T.A.: 1981, *Astrophys. J.* **244**, 1064
Ayres, T.A., Testerman, L.: 1981, *Astrophys. J.* **245**, 1124
Ayres, T.A., Testerman, L., Brault, J.W.: 1986, *Astrophys. J.* **304**, 542
Bray, R.J., Loughhead, R.E., Durrant, C.J.: 1984, *Solar Granulation*, 2nd ed., Cambridge Univ. Press, Cambridge
Deming, D., Hillman, J.J., Kostiuk, T., Mumma, M.J.: 1984, *Solar Phys.* **94**, 57
Gustafsson, B., Bell, R.A., Eriksson, K., Nørdlund, Å.: 1975, *Astron. Astrophys.* **42**, 407
Heasley, J.N., Ridgway, S.T., Carbon, D.F., Milkey, R.W., Hall, D.N.B.: 1978, *Astrophys. J.* **219**, 970
Johnson, H.R.: 1973, *Astrophys. J.* **180**, 81
Kalkofen, W., Ulmschneider, P.: 1977, *Astron. Astrophys.* **57**, 193
Kirby-Docken, K., Liu, B.: 1978, *Astrophys. J. Suppl.* **36**, 359
Kneer, F.: 1983, *Astron. Astrophys.* **128**, 311
Kurucz, R.L.: 1979, *Astrophys. J. Suppl.* **40**, 1
Kurucz, R.L., Avrett, E.H.: 1981, *Smithsonian Astrophys. Obs. Spec. Rep. No.* 391
Mantz, A.W., Maillard, J.-P., Roh, W.B., Rao, K.N.: 1975, *J. Molec. Spectr.* **57**, 155
Muchmore, D.: 1986, *Astron. Astrophys.* **155**, 172
Muchmore, D., Ulmschneider, P.: 1985, *Astron. Astrophys.* **142**, 393
Schmitz, F., Ulmschneider, P., Kalkofen, W.: 1985, *Astron. Astrophys.* **148**, 217
Steffen, M., Muchmore, D.: 1988, *Astron. Astrophys.* **193**, 281
Tsuji, T.: 1968, in Colloq. on *Late Type Stars*, M. Hack, ed., Osservatorio Astronomico di Trieste, p. 260
Ulmschneider, P., Kalkofen, W., Nowak, T., Bohn, H.U.: 1977, *Astron. Astrophys.* **54**, 61
Ulmschneider, P., Schmitz, F., Kalkofen, W., Bohn, H.U.: 1978, *Astron. Astrophys.* **70**, 487